

Domain Generalization with Correlated Style Uncertainty

Zheyuan Zhang^{1,2}, Bin Wang^{1,2}, Debesh Jha², Ugur Demir², Ulas Bagci^{1,2}

¹ Department of Biomedical Engineering, Northwestern University

² Department of Radiology, Northwestern University

ulas.bagci@northwestern.edu

Abstract

Domain generalization (DG) approaches intend to extract domain invariant features that can lead to a more robust deep learning model. In this regard, style augmentation is a strong DG method taking advantage of instance-specific feature statistics containing informative style characteristics to synthetic novel domains. However, prior works on style augmentation have disregarded the interdependence amongst distinct feature channels or have solely constrained style augmentation to linear interpolation. In this work, we introduce a cutting-edge augmentation approach named *Correlated Style Uncertainty (CSU)*, which surpasses the limitations of linear interpolation in style statistic space and simultaneously preserves vital correlation information. Our method's efficacy is established through extensive experimentation on diverse cross-domain computer vision and medical imaging classification tasks, namely PACS, Office-Home, and Camelyon17 datasets, as well as the Duke-Market1501 instance retrieval task. The results showcase a remarkable improvement margin over existing state-of-the-art techniques. The source code is available for public use.

1. Introduction

Recent years have witnessed the remarkable success of Deep learning (DL) in computer vision when following the assumption that the source data for training and the target data for testing share an independent and identical distribution (iid) [47]. This oversimplified assumption often fails in practice when the distribution drift between training and testing exists. The violation of this assumption induces the phenomenon that well-trained model in the source domain degrades dramatically in the target domain. Achieving the domain generalization property of a DL model would result in an automatic resolution of domain shift issues, provided that the former is successfully attained. This would not only signify a significant advancement in the field, but also streamline the practical deployment of DL models across various domains. For example, a car detector should per-

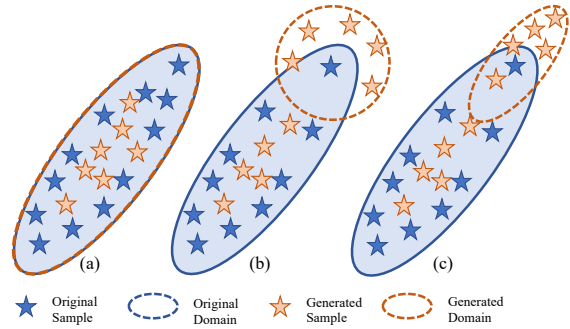


Figure 1. Visualization of synthetic feature statistics samples using (a) MixStyle [49], (b) DSU [21], and (c) Our proposed Correlated Style Uncertainty (CSU) methods. The proposed strategy (CSU) goes beyond the linear interpolation while preserving the correlation among feature channels.

form accurately both on sunny and cloudy days. DL based medical image segmentation algorithm, for another example, should generate stable segmentation regardless of the acquisition and scanner differences, and so on.

Domain adaptation and **domain generalization** are two distinct approaches for addressing the challenge of domain shift in machine learning. A prevailing solution for mitigating domain shift issues involves collecting unlabeled data from the target domain and adapting a model trained on the source domain to the target domain using this data. This strategy is called Domain Adaptation (DA), which has been the subject of much systematic investigation in the last few years and achieved promising results in many fields [47]. To ensure robust model adaptation, regularization algorithms such as entropy regularization [28, 31] are also applied to target domain during training. Domain adaptation assumes that the target domain is known and that some data from the target domain is available for training. However, accessing the target domain data can be quite challenging. Specifically in high-risk applications (i.e., medical data), target domain data might not be available at all. This is a primary research concern of Domain Generalization (DG) as a

strong alternative path to DA, hence.

In DG, the objective is to develop models that can perform well across a wide range of domains without explicit training on each individual domain. Unlike DA, DG assumes that the target domain is unknown and that no data from the target domain is available for training [38, 47]. As target data is unavailable for investigating domain shift, DG relies solely on extracting robust, domain-invariant feature representations from diverse training distributions. As a result, when domain information is feasible, feature alignments among different domains could significantly leverage the model’s out-of-distribution generalization ability, as shown in previous research [4, 20, 23].

What do we propose? In this paper, we propose a novel DG method, called Correlated Style Uncertainty (CSU), to preserve the correlation between different feature space channels while addressing the distribution drift between target and source domains, as demonstrated in Figure 1(c) compared with MixStyle and DSU, two popular methods. Similar to these two methods, our proposed algorithm CSU is also a member of style augmentation methods within DG but with clear distinction and benefits. For augmentation, briefly, MixStyle randomly selects two samples and conduct linear interpolation between the corresponding style characteristics. Although it is useful, it can only produce in-distribution samples, potentially limiting the generalization capabilities of any network. DSU, on the other hand, can alleviate this drawback by generating out-of-distribution samples via an uncertainty modeling of feature statistics. However, it relies on the assumption that each channel is independent and the correlation among channels has no influence on the given tasks.

Our proposed method, CSU, is fundamentally different from these two methods because i) it produces out-of-distribution samples, and ii) correlation among different channels are not ignored. In other words, we are addressing the current weaknesses of both DSU and MixStyle with our innovative solution. As a result, CSU enables us to generate more reasonable style perturbation in discriminative tasks and increase model’s generalization ability. As in previous research, we hold the hypothesis that the feature statistics follow a multivariate Gaussian distribution, but there exists a correlation between each variate. Specifically, we first calculate the covariance matrix on the mini-batch level and then estimate the distribution from the covariance matrix. Then, the correlated feature statistics can be sampled from the calculated distribution. This sampling allows us to generate the style statistics outside the linear interpolation while maintaining an identical correlation. With this way, more diverse but meaningful style augmentation can be applied during the training and increase the model’s generalization ability. We highlight our main contributions in this study as follows:

- Our proposed strategy (CSU) is a well-calibrated framework that goes beyond the interpolation strategies by preserving correlation between different feature spaces. This allows us to generate more diverse and meaningful style augmentation during training which helps in building a more generalizable model. To the best of our knowledge, such a simple yet effective style augmentation strategy has never been explored before.
- To evaluate the effectiveness of the proposed CSU model, we conducted extensive experiments on multi-domain classification benchmarking datasets, including PACS [18], Office-Home [34], Camelyon17 [1] and the Duke-Market1501 dataset for instance retrieval tasks [30, 45]. The quantitative experimental results show that the CSU model can significantly improve the model’s generalizability over other state-of-the-art (SOTA) methods.
- We have performed several ablation studies to investigate the optimal position to insert CSU model, optimal sampling hyperparameters, and batch size leading to a better generalization.

2. Background and Related Works

Several DG strategies have been proposed in the literature; we briefly cover the mostly used ones under sub-categories as follows.

Data Augmentation: is widely regarded for enabling the model to effectively encounter a greater volume of samples, an essential element for successful Deep Learning. As a consequence, the model is compelled to extract domain-invariant features to effectively address variance transforms occurring during the training process. Many methods have been proposed to achieve strong data augmentation, including traditional image augmentation like BigAug [22, 42], deep neural network-based image generation like in Rand-Conv [39], and adversarial data augmentations [29, 36]. These methods are suitable specifically when the domain tags of samples are agnostic. While data augmentation is a powerful technique that can improve the generalization performance of machine learning models, it also has some potential drawbacks in the context of domain generalization. For instance, one drawback is that data augmentation may introduce unrealistic or irrelevant variations in the training data. Another drawback is it may not be effective when the variations between the source and target domains are too significant.

Feature Alignment: is a popular method in representation learning category of DG approaches. Given domain tags, the model will add regularization terms into loss functions to force the extracted features from all source domains

to align to the same distribution [4, 8, 20, 23, 37]. For instance, Li [19] introduced the Maximum Mean Discrepancy as a regularization term to achieve feature alignment across multiple domains. Zhao [44] proposed an entropy regularization term that measures the dependency between the learned features and corresponding labels. This regularization method can ensure the conditional invariance of learned features. While feature alignment has shown promising results in some applications, it also has some potential drawbacks. One major drawback is that it can be difficult to determine the best way to align the features across domains.

Meta-learning: has also attracted attention from DG communities [2, 5, 7, 17, 33]. Meta-learning aims to learn the learning algorithm itself by learning from previous experience or tasks. By splitting the source domain samples into pseudo-train and pseudo-test, meta-learning mimics the potential domain shift of the actual target domain. Thus, by minimizing the loss using pseudo-test data, the meta-learning forces the model to extract more domain-invariant features. Despite its promise, meta-learning can be computationally expensive and time-consuming. Further, since meta-learning involves training a model on a large number of tasks or domains, there is a risk that the model may overfit to the training data and not generalize well to new domains.

Style Augmentation: The final category of DG is very recent: *style augmentation*. This method comes from the simple observation that instance-specific feature statistics such as mean and standard deviation, contain informative style characteristics and can be applied to the style-transferring model [13]. This phenomenon allows us to generate different style images while maintaining the same semantic concept. Zhou et al. [49] presented mixing styles (MixStyle) of training instances, and increased the source domain diversity. As a result, authors leveraged the trained model’s generalizability. Nuriel et al. [26] alternatively proposed a Permuted Adaptive Instance Normalization (pAdaIN) method to rearrange the instance-specific feature statistics within a batch, thus improving the model’s generalizability. In a slightly different angle, Li et al. [21] quantified feature statistics’ uncertainty (DSU) and sampled new style feature statistics from the uncertainty distribution, resulting in novel out-of-distribution domains being synthesized implicitly. Our work is related to MixStyle and DSU, and some similarities with pAdaIN, from the same efforts for synthesizing novel domains, but our proposed CSU generates out-of-distribution feature statistics while maintaining the correlation between features.

3. Methods

3.1. Correlation within the style statistics

Given batch level feature maps $x \in \mathbb{R}^{B \times C \times H \times W}$ of the network $f(in, \phi)$ where in denotes the batch-wise inputs

and ϕ denotes the network parameters. We can formulate the instance-specific feature statistics mean $\mu \in \mathbb{R}^{B \times C}$ and standard deviation $\sigma \in \mathbb{R}^{B \times C}$ as follows

$$\mu(x) = \frac{1}{HW} \sum_{h=1}^H \sum_{w=1}^W x_{b,c,h,w}, \quad (1)$$

$$\sigma^2(x) = \frac{1}{HW} \sum_{h=1}^H \sum_{w=1}^W (x_{b,c,h,w} - \mu(x))^2. \quad (2)$$

Thus, we can further formulate the channel-wise covariance matrix $\Sigma_\mu \in \mathbb{R}^{C \times C}$, $\Sigma_\sigma \in \mathbb{R}^{C \times C}$ of μ, σ :

$$\Sigma_\mu = \frac{1}{B} (\mu - E(\mu))^T (\mu - E(\mu)), \quad (3)$$

$$\Sigma_\sigma = \frac{1}{B} (\sigma - E(\sigma))^T (\sigma - E(\sigma)), \quad (4)$$

where $E(\mu), E(\sigma)$ represents the mean value of μ, σ over batch dimension. It is worth noting that the rank of $\Sigma_\mu, \Sigma_\sigma$ is strictly limited by $\min(B, C) \leq C$. Many previous research studies already indicated that the feature maps can hardly be linear independent over the channel dimension [12, 43]. This phenomenon has been widely applied to reduce the size of the network without reducing its performance [11]. Thus, we can hardly assume that the covariance matrix is diagonal and the correlation between each channel is zero without applying any regularization as shown in the upper row of Figure 2.

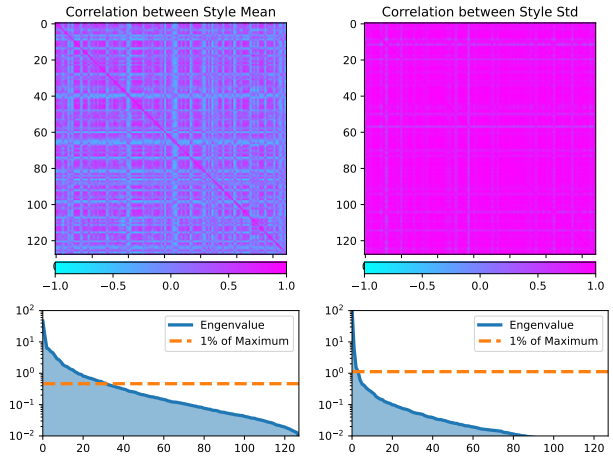


Figure 2. Visualization of feature statistics correlation. We calculate the style statistics (mean and standard deviation, respectively) on the PACS dataset. We extract the feature using the second residual block output from the ImageNet pretrained on ResNet18 [9] with a channel size of 128. For 4 domains of the PACS dataset, including Art, Cartoon, Photo, and Sketch, we select 64 cases from every category (7 categories in total) under each domain. Therefore, the data samples to calculate the correlation matrix is $7 \times 4 \times 64 = 1792 \gg 128$.

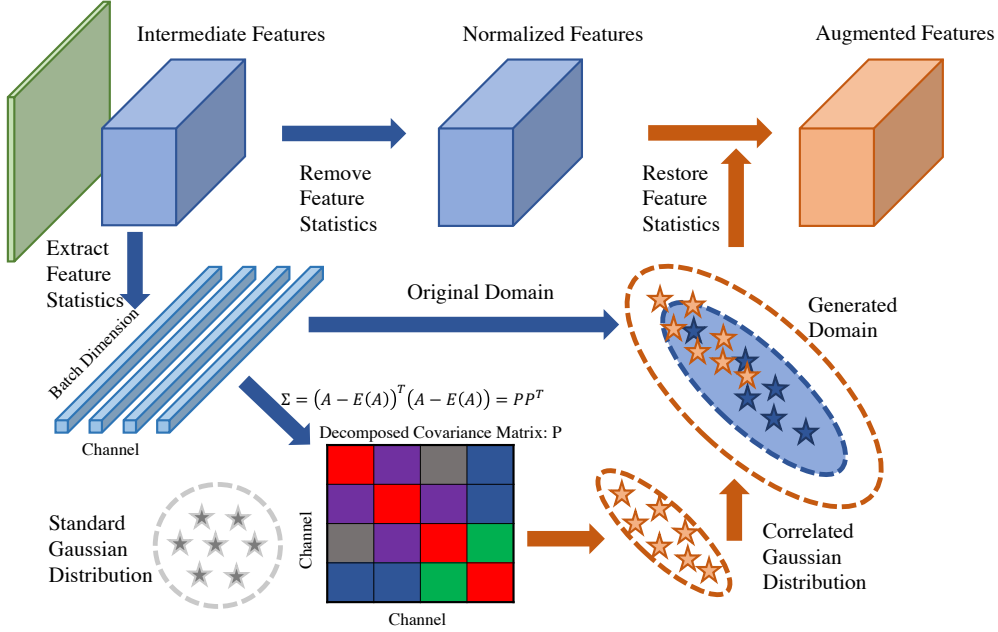


Figure 3. Visualization of feature statistics augmentation using correlated style uncertainty (CSU). Given the intermediate features extracted from the network, we first estimate the covariance matrix of feature statistics and decompose the covariance matrix as described in Sec 3.2. Based on this decomposition, we could generate correlated augmentation from the standard Gaussian distribution that shares identical distribution as the original domain. Then, we update raw data feature statistics by adding this correlated augmentation. Finally, we restore the feature statistics back to the normalized features and achieve the augmented features.

We observe that the correlation matrix of style statistics (regardless of the mean or the standard deviation values) is not diagonal, and there exists a strong correlations among channels. Furthermore, we apply eigenvalue decomposition over the calculated correlation matrix and find that very few eigenvectors dominate most variance, as shown in the bottom row of the Figure 2. This inspires us to rethink the augmentation of style statistics. The correlation matrix indicates that the combinations of feature statistics are not arbitrary but limited by task objectives and training procedures. Additionally, most variances happen within specific principal directions. Arbitrary augmentation over the style statistics might damage the training itself. Previous research about why InstanceNorm can not outperform the BatchNorm in the discriminative tasks also proves this finding [24].

Based on this observation, we revisit the central question about feature statistics augmentation. MixStyle [49] adopts a linear interpolation within instance-level feature (statistics) space and preserves the channel(s) information. pAdaIN [26] permutes the order of feature statistics and preserves the information from the channel combination. However, these two methods limit the augmentation within the original feature (statistics) space. DSU [21] attempts to go beyond the interpolation between training samples using uncertainty quantification. However, this calculation relies on the assumption that the feature statistics of every channel

are strictly orthogonal. Thus, correlated uncertainty quantification can effectively generate feature statistics out of the training domain while preserving the correlation between channels. This is crucial to generate more reasonable feature statistics/ augmentation than ever before. Our proposed CSU addresses the aforementioned challenges and drawbacks of feature statistics by generalizing the interpolation-based strategies under correlation assumption.

3.2. Modeling correlated style uncertainty

Given that the correlation matrix is real, symmetric, and positive semi-definite, we can always apply eigenvalue decomposition on $\Sigma_\mu, \Sigma_\sigma$ to analyze its subspaces as:

$$\Sigma_\mu = Q_\mu \text{diag}(\Lambda_\mu) Q_\mu^T, \quad (5)$$

$$\Sigma_\sigma = Q_\sigma \text{diag}(\Lambda_\sigma) Q_\sigma^T, \quad (6)$$

$$Q_\mu Q_\mu^T = Q_\sigma Q_\sigma^T = I, \quad (7)$$

$$\Lambda_\mu, \Lambda_\sigma \in \mathbb{R}^C, Q_\mu, Q_\sigma \in \mathbb{R}^{C \times C}, \quad (8)$$

where $\Lambda_{\mu,i} \geq \Lambda_{\mu,j} \geq 0$, $\Lambda_{\sigma,i} \geq \Lambda_{\sigma,j} \geq 0$ ($i > j$) represent the sorted eigenvalues, Q_μ, Q_σ represent the corresponding eigenvectors. The eigenvector corresponding to the largest eigenvalue represents the direction that we could apply dense augmentation. Eigenvectors corresponding to the eigenvalues of 0 or close to 0 are not considered in the data augmentation process due to low variance across such directions within the dataset.

We assume that the μ, σ still follows the multi-variable Gaussian distribution with k_μ, k_σ represents the independent variable number (or the rank of the corresponding covariance matrix), we could represent the probability distribution function as:

$$f_\mu = \frac{1}{(2\pi)^{k_\mu} \det^*(\Sigma_\mu)} \exp^{-(\mu - E(\mu))^T \Sigma_\mu^+ (\mu - E(\mu))}, \quad (9)$$

$$f_\sigma = \frac{1}{(2\pi)^{k_\sigma} \det^*(\Sigma_\sigma)} \exp^{-(\sigma - E(\sigma))^T \Sigma_\sigma^+ (\sigma - E(\sigma))}, \quad (10)$$

where the \det^* is the pseudo-determinant and Σ^+ is the generalized inverse. Based on this distribution function, we could further derive the correlated uncertainty augmentation after we sample $\epsilon_\mu, \epsilon_\sigma \in \mathbb{R}^{N \times C}$ from the standard Gaussian distribution $Y \sim \mathcal{N}(0, I)$ as follow:

$$P_\mu = Q_\mu \text{diag}(\Lambda_\mu)^{\frac{1}{2}} Q_\mu^T, \quad (11)$$

$$P_\sigma = Q_\sigma \text{diag}(\Lambda_\sigma)^{\frac{1}{2}} Q_\sigma^T, \quad (12)$$

$$\hat{\epsilon}_\mu = \epsilon_\mu P_\mu, \quad \hat{\epsilon}_\sigma = \epsilon_\sigma P_\sigma. \quad (13)$$

Essentially, we determine the transform matrix P such that the covariance matrix $\Sigma = PP^T$ as shown in Eq.11-12, and these transformation matrices allow us to maintain the correlation. We sample the correlated perturbations $\hat{\epsilon} \in \mathbb{R}^{N \times C}$ from independent Gaussian noise $\epsilon \in \mathbb{R}^{N \times C}$ as shown in Eq.13. Note the covariance matrix:

$$\begin{aligned} \Sigma = PP^T &= Q \text{diag}(\Lambda_\mu)^{\frac{1}{2}} Q^T (Q \text{diag}(\Lambda_\mu)^{\frac{1}{2}} Q^T)^T \\ &= Q \text{diag}(\Lambda_\mu)^{\frac{1}{2}} (Q \text{diag}(\Lambda_\mu)^{\frac{1}{2}})^T \end{aligned}$$

Therefore, these two transformations $Q \text{diag}(\Lambda_\mu)^{\frac{1}{2}} Q^T$, $Q \text{diag}(\Lambda_\mu)^{\frac{1}{2}}$ both work in principle. However, in practice, if we use the standard format of eigen-decomposition, stochastic axis swapping in the eigenvector will not influence this decomposition, but it can lead to unstable training. Thus, we apply the decomposition trick in the format of $Q \text{diag}(\Lambda_\mu)^{\frac{1}{2}} Q^T$ rather than using only one set of eigenvectors $Q \text{diag}(\Lambda_\mu)^{\frac{1}{2}}$ to avoid the random flip issue in traditional eigenvalue decomposition [12]. Finally, although we sample $\epsilon_\mu, \epsilon_\sigma$ from C independent normal variables, the finally generated $\hat{\epsilon}_\mu, \hat{\epsilon}_\sigma$ has only k_μ, k_σ independent components, corresponding to non-zero eigenvalue components.

3.3. Style augmentation with CSU

Based on the previous two sections, we now present the style augmentation with correlated style uncertainty as follow:

$$\beta(x) = \mu(x) + \lambda * \hat{\epsilon}_\mu, \quad (14)$$

$$\gamma(x) = \sigma(x) + \lambda * \hat{\epsilon}_\sigma, \quad (15)$$

where $\lambda \sim \text{Beta}(\alpha, \alpha)$ represents the augmentation intensity generated from the Beta distribution. Hyperparameter

α controls the shape of the distribution. In the ablation experiments, we further show the influence of hyperparameter selections on the final performance. We can understand the equation in one more intuitive way, the first part is to provide in-domain samples to cover the whole training domain, and the second is to provide the extrapolation while maintaining the same data distribution.

$$\beta(x) = \underbrace{\mu(x)}_{\text{In Domain Sample}} + \underbrace{\lambda * \hat{\epsilon}_\mu}_{\text{Out Domain extrapolation}}$$

The final augmented instance feature can be defined as:

$$CSU(x) = \gamma(x) \left(\frac{x - \mu(x)}{\sigma(x)} \right) + \beta(x). \quad (16)$$

This plug-and-play module can be easily inserted into any current framework. We further provide one PyTorch-like pseudo-code in the supplementary materials.

4. Experiments

4.1. Multi-domain Classification Tasks

We validate our model's performance on various multi-domain classification tasks, including PACS, Office-Home, and Camelyon17. Figure 4 shows some examples with observable domain shifts within the same class. In all experiments, the domain tags are agnostic. Following the MixStyle, we adopt the ResNet-18 [10] with ImageNet [6] pre-training as the backbone for classification. We follow the Leave-One-Domain-Out strategy, which leaves one domain out for evaluation and the rest of the domains participating in the training. We adopt the widely used multi-domain classification framework proposed by Zhou [47] for a fair comparison. The batch size is set as 64. We conduct all the experiments on 2 NVIDIA A6000 GPU based on PyTorch [27] framework.



Figure 4. Some examples from multi-domain classification including (a) PACS, (b) Office-Home, and (c) Camelyon17 dataset.

4.1.1 PACS classification

PACS [18] is a widely used benchmark dataset for DG, which contains four domains: Photo (1,670 images), Art Painting (2,048 images), Cartoons (2,344 images), and Sketches (3,929 images). Each domain consists of seven categories for classification tasks. These domain shifts are

Method	Reference	Art	Cartoon	Photo	Sketch	Average(%)
Baseline	-	74.3	76.7	96.4	68.7	79.0
Mixup [41]	ICLR 2018	76.8	74.9	95.8	66.6	78.5
Manifold Mixup [35]	ICML 2019	75.6	70.1	93.5	65.4	76.2
CutMix [40]	ICCV 2019	74.6	71.8	95.6	65.3	76.8
JiGen [3]	CVPR2019	79.4	75.3	96.0	71.6	80.5
RSC [14]	ECCV 2020	78.9	76.9	94.1	76.8	81.7
L2A-OT [48]	ECCV 2020	83.3	78.2	96.2	76.3	82.8
SagNet [25]	CVPR 2021	83.6	77.7	95.5	76.3	83.3
pAdaIN [26]	CVPR 2021	81.7	76.6	96.3	75.1	82.5
MixStyle [49]	ICLR 2021	82.3	79.0	96.3	73.8	82.8
DSU [21]	ICLR 2022	83.6	79.6	95.8	77.6	84.1
CSU (Ours)	-	85.0	81.0	96.3	78.4	85.2

Table 1. Experimental results on the PACS multi-domain classification task. CSU achieves around highly significant improvements over the baseline in Art, Cartoon, and Sketch domains, respectively, as: 14.3%, 5.6%, and 12.2%. Besides, CSU also shows superiority over other methods, which demonstrates its effectiveness. α is set as 0.1.

highly suitable for validating the effectiveness of the DG algorithms. Here, we compare our model’s performance with other SOTA methods, and all the evaluation metrics indicate the reported value by default.

The experiment results, as shown in Table 1, indicate a significant improvement over other methods, proving the effectiveness of the CSU: notably, 14.3%, 5.6%, 12.2%, over the baseline in the Art, Cartoon, and Sketch domains, respectively. Overall, CSU has a nearly 7.8% improvement in average accuracy across four domains. Given that we adopted the pre-trained model on ImageNet, it would be hard to generate significant improvement over the baseline in the Photo domain (As discussed in [39]), as this is expected. Nevertheless, we can still preserve the most dominant features by taking advantage of correlation modeling. Consequently, we achieve a minimum performance drop (around 0.1%) compared with other methods. Furthermore, to guarantee the reliability of the reported value, we conduct training stability analysis in the supplementary materials.

4.1.2 Office-Home classification

Office-Home [34] is another benchmark dataset for DG, containing four domains: Art, Clipart, Product, and Real-World, and each domain consists of 65 categories. The dataset contains 15,500 images with an average of around 70 photos per class. Similarly, we compare our model’s performance with other SOTA methods.

As shown in Table 2, CSU achieves around 4.3%, 13.6%, 0.9% improvement over the baseline in Art, Clipart, and Product domain, respectively. For the same reason, improving the Real-world images in the PACS dataset is hard. However, CSU remains with a strong performance with only 0.1% drop. On average, CSU shows 3.7% improvement over the baseline across four domains.

4.1.3 Camelyon17 classification

Medical image analysis often suffers the most from domain shifting, given that multiple parameters, like the im-

Method	Art	Clipart	Product	Real	Average(%)
Baseline	58.8	48.3	74.2	76.2	64.4
Mixup [41]	58.2	49.3	74.7	76.1	64.6
CrossGrad [32]	58.4	49.4	73.9	75.8	64.4
Manifold Mixup [35]	56.2	46.3	73.6	75.2	62.8
CutMix [40]	57.9	48.3	74.5	75.6	64.1
RSC [14]	58.4	47.9	71.6	74.5	63.1
L2A-OT [48]	60.6	50.1	74.8	77.0	65.6
MixStyle [49]	58.7	53.4	74.2	75.9	65.5
DSU [21]	60.2	54.8	74.1	75.1	66.1
CSU (Ours)	61.3	54.9	74.9	76.1	66.8

Table 2. Experimental results on Office-Home multi-domain classification task. We achieve around 4.3%, 13.6%, 0.9% improvement over the baseline in the Art, Clipart, and Product domain, respectively. CSU consistently outperforms the other strong baseline models with considerable margins ($\alpha = 0.4$)

Method	H1	H2	H3	H4	H5	Average(%)
Baseline	95.3	91.4	89.5	96.2	94.6	93.4
MixStyle [49]	96.1	91.2	93.0	95.0	92.7	93.6
pAdaIN [26]	96.6	93.0	94.7	95.2	94.0	94.7
DSU [21]	96.8	93.3	91.7	96.4	94.4	94.5
CSU (Ours)	96.7	93.8	94.2	95.5	95.5	95.1

Table 3. Experimental results on Camelyon17 multi-domain classification task. H1-H5 represents five different hospitals. We can find that CSU outperforms other methods ($\alpha = 0.3$).

age acquisition device, and protocol can induce significant domain shift. We validate the model’s performance on the challenging Camelyon17 dataset [1], containing images from five medical centers. This dataset consists of the histopathological images as input and the labels indicating whether the central region includes any tumor tissue. Due to lacking reported performance from the current literature, we conduct this experiment from scratch based on the WILDS framework proposed by Koh [16]. Besides the baseline, we compare our model with three state-of-art strategies, including the MixStyle [49], pAdaIN [26], DSU [21]. For a fair comparison, we directly use the official implementation of

Model		Market	To	Duke		Duke	To	Market
ResNet-50	mAP	R1	R5	R10	mAP	R1	R5	R10
Baseline	19.3	35.4	50.4	56.4	20.4	45.2	63.6	70.9
RandomErase [46]	14.3	27.8	42.6	49.1	16.1	38.5	56.8	64.5
DropBlock [49]	18.2	33.2	49.1	56.3	19.7	45.3	62.1	69.1
MixStyle [49]	23.8	42.2	58.8	64.8	24.1	51.5	69.4	76.2
pAdaIN [26]	22.0	41.4	56.4	62	24.1	52.1	68.8	75.5
DSU [21]	21.2	40.5	56	62.5	24.0	51.7	70.6	77.3
CSU (Ours)	24.5	44.1	60.3	65.9	24.4	52.4	71.4	78.2
OSNet	mAP	R1	R5	R10	mAP	R1	R5	R10
Baseline	25.9	44.7	59.6	65.4	24.0	52.2	67.5	74.7
RandomErase [46]	20.5	36.2	52.3	59.3	22.4	49.1	66.1	73.0
DropBlock [49]	23.1	41.5	56.5	62.5	21.7	48.2	65.4	71.3
MixStyle [49]	27.2	48.2	62.7	68.4	27.8	58.1	74.0	81.0
pAdaIN [26]	28.3	48.8	62.7	68.1	27.6	57.5	74.2	80.3
DSU [21]	29.0	51.0	65.0	70.4	26.1	57.2	74.6	80.7
CSU (Ours)	31.1	53.1	67.9	76.3	29.8	60.1	77.3	83.4

Table 4. Experimental results on the Duke-Market1501 Instance Retrieval Datasets. CSU achieves around 26.9%, 19.6% advancement over the baseline in mAP value using the ResNet-50 model in the Market1501 to Duke and the Duke to Market1501 experiment, correspondingly. Likewise, CSU achieves around 20.1%, 24.2% improvement for the OSNet model experiment. We could also observe similar advancements in ranking accuracy, and CSU achieves impressive improvement over other methods.

each method without any modifications.

Table 3 proves the effectiveness of our model. CSU achieves impressive improvement compared with the baseline or other style augmentation methods. This indicates that by taking advantage of correlation modeling, CSU can help induce a more generalized model even with extremely challenging medical data.

4.2. Instance Retrieval Experiments

The person re-identification problem aims to match a person across multi-camera views, and the image coming from each disjoint camera can be considered as one independent domain. Thus, the person re-identification problem is a challenging DG problem. Following previous research, we conducted this experiment on the commonly used Duke [30] and Market1501 [45] datasets. To evaluate the model’s generalizability, we take one dataset as training and test the performance on the other domain. The camera data from the test domain will not participate in any training process. We adopt the exact framework implementation of MixStyle and test the CSU influence on the ResNet50 [10] and OSNet [48]. Similarly, ranking accuracy and mean average precision (mAP) are performance measures. For a fair comparison, we repeat the pAdaIN and DSU experiments on the same framework with the MixStyle and use the best configuration reported in the original paper.

Table 4 shows the experiment results using two models in the two domains. We could observe that CSU outperforms other methods by a large margin. CSU achieves around 26.9%, 19.6% advancement in mAP using the ResNet-50 model in the Market1501 to Duke and the

Duke to Market1501 experiment, correspondingly. Similarly, CSU achieves around 20.1%, 24.2% improvement for the OSNet model experiment. We could also observe similar advancements in ranking accuracy, and CSU achieves impressive improvement over other methods. Nevertheless, to show the effectiveness of CSU rather than position fine-tuning, we insert the permutation in all positions as described in Sec 4.3. The supplementary materials show that changing the inserting position can achieve even more significant performance advancement.

4.3. Ablation Experiments

Insert Position Selection: To answer the question of where we should insert the CSU, we conduct comprehensive experiments on the PACS and Office-Home datasets using the ResNet18 structure. We investigate all possible positions of ResNet18, including the first Convolution, first Max Pooling, and 1, 2, 3, and 4 Res-block, which are named 0-5, respectively. We divide the experiment into several groups according to the inserted CSU number. Within each group, we shift the start position one by one from 0 to end. For example, for the group containing 2 CSU blocks, we will have 01, 12, 23, 34, and 45 potential combinations and five comparison experiments in total. To avoid the influence of hyperparameters, we set $\alpha = 0.3$ for all experiments. Thus, we can reasonably and adequately compare the inserting position’s influence on final performance.

Figure 5 shows the ablation experiment results. Inserting 6 blocks of CSU in all potential positions achieves the best results for the PACS dataset while inserting 4 blocks of CSU in the last 4 positions achieves the best results for the Office-

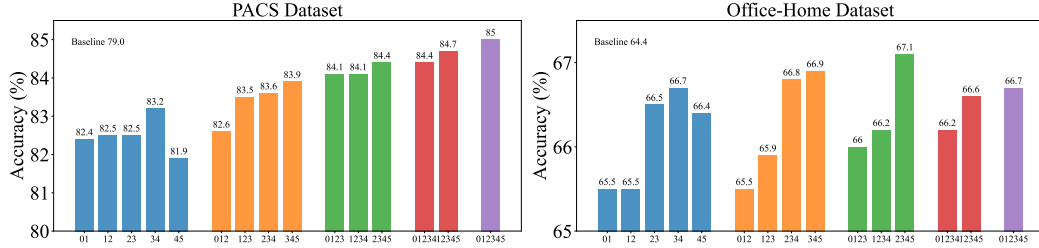


Figure 5. Influence of inserting position. Inserting 6 blocks of CSU in all potential positions achieves the best results for the PACS dataset while for the Office-Home dataset, inserting 4 blocks of CSU in the last 4 positions achieves the best results. The performance after inserting the CSU model always shows superiority over the baseline by a large margin regardless of the inserting number or position.

Home dataset. Within each group of a fixed number of CSU blocks, the performance tends to increase when we start the inserting position at the medium blocks. This trend is different with the MixStyle which the model prefers the first several blocks [49]. We explain this phenomenon as CSU can provide more reasonable feature (statistics) augmentation due to correlation preservation. This preservation will avoid information loss in the medium or last blocks. We can also notice that compared with inserting 4, 5, and 6 blocks of CSU, inserting 2, or 3 blocks of CSU can not achieve comparable performance. This indicates that a more significant number of CSU blocks can be helpful to increase the model’s generalization ability due to accumulated correlations over the blocks. It is also worth noting that no matter how we choose the inserting position, the performance of the CSU model always shows superiority over the baseline by a large margin. This firmly proves the effectiveness of the proposed model.

Hyper-parameter Selection: As described in the previous section, the hyper-parameter alpha determines the intensity of augmentation during training by manipulating the shape of the Beta distribution. Here, we show the influence of alpha on the PACS, Office-Home using the ResNet18 structure. Similarly, to avoid the influence of different inserting positions, we insert CSU block in all positions for every experiment. We select α from 0.1, 0.2, 0.3, 0.4, 0.5, 0.7, and 0.9 for one comprehensive experiment. As shown in Figure 6, we can find that a smaller number of $\alpha < 0.5$ always performs better than the relatively larger number (> 0.5). Based on these experiment results, we recommend selecting the alpha from 0.1, 0.2, 0.3, and 0.4, and the best configuration may vary according to the tasks.

Effect of Batch Size: Different batch sizes can influence estimating correlation information; hence, it is essential to investigate the influence of batch size on the final generalizability. Here, we insert the CSU in every position like in the previous section and fix $\alpha = 0.3$ for each experiment. We compare the model’s performance with a batch size of 16, 32, 64, 128, 256, and 512. Figure 7 shows the experimental result. We found that it might be hard to estimate an accurate correlation when the batch size is too small. Sim-

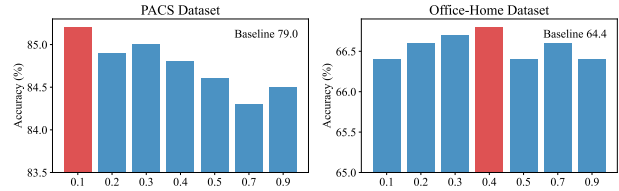


Figure 6. Influence of hyper-parameters selection. We can find that a smaller number of $\alpha < 0.5$ always performs better than the relatively larger number (> 0.5). Red indicates the best result.

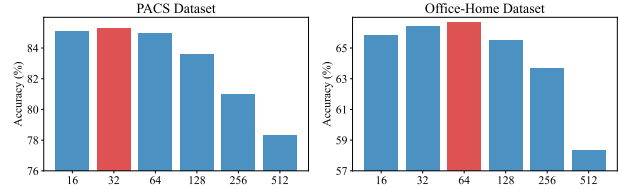


Figure 7. Effect of batch size on the two classification tasks. It shows that too small or too large batch size can potentially be toxic for DG. Red indicates the best result.

ilarly, when the batch size is too large, the network tends to converge to sharp minimizers of the training and testing functions, leading to poorer generalizations, as shown in previous research [15].

5. Conclusion

In summary, we proposed one Correlated Style Uncertainty (CSU) to go beyond linear interpolation while preserving the correlation between feature channels. CSU allows us to generate more diverse and meaningful style augmentation during training which helps in building a generalizable model. We provide careful and extensive ablation studies, which indicate the suitable position for inserting the CSU model, the influence of sampling hyperparameters, and the selection of batch size to achieve a more generalized model. Comprehensive experiment results on various datasets effectively prove that the CSU model can significantly improve the model’s generalization ability. We anticipate that this research can lead to more thorough studies about feature statistics augmentation in the future.

References

- [1] Peter Bandi, Oscar Geessink, Quirine Manson, Marcorry Van Dijk, Maschenka Balkenhol, Meyke Hermesen, Babak Ehteshami Bejnordi, Byungjae Lee, Kyunghyun Paeng, Aoxiao Zhong, et al. From detection of individual metastases to classification of lymph node status at the patient level: the camelyon17 challenge. *IEEE Transactions on Medical Imaging*, 38(2):550–560, 2018. 2, 6
- [2] Manh-Ha Bui, Toan Tran, Anh Tran, and Dinh Phung. Exploiting domain-specific features to enhance domain generalization. *Advances in Neural Information Processing Systems (NIPS)*, 34:21189–21201, 2021. 3
- [3] Fabio M Carlucci, Antonio D’Innocente, Silvia Bucci, Barbara Caputo, and Tatiana Tommasi. Domain generalization by solving jigsaw puzzles. In *Proceedings of the IEEE/CVF Conference on Computer Vision and Pattern Recognition (CVPR)*, pages 2229–2238, 2019. 6
- [4] Yining Chen, Elan Rosenfeld, Mark Sellke, Tengyu Ma, and Andrej Risteski. Iterative feature matching: Toward provable domain generalization with logarithmic environments. *arXiv preprint arXiv:2106.09913*, 2021. 2, 3
- [5] Seokeon Choi, Taekyung Kim, Minki Jeong, Hyoungseob Park, and Changick Kim. Meta batch-instance normalization for generalizable person re-identification. In *Proceedings of the IEEE/CVF conference on Computer Vision and Pattern Recognition (CVPR)*, pages 3425–3435, 2021. 3
- [6] Jia Deng, Wei Dong, Richard Socher, Li-Jia Li, Kai Li, and Li Fei-Fei. Imagenet: A large-scale hierarchical image database. In *2009 IEEE conference on computer vision and pattern recognition*, pages 248–255, 2009. 5
- [7] Yingjun Du, Xiantong Zhen, Ling Shao, and Cees GM Snoek. Metanorm: Learning to normalize few-shot batches across domains. In *Proceedings of the International Conference on Learning Representations (ICLR)*, 2020. 3
- [8] Cian Eastwood, Alexander Robey, Shashank Singh, Julius von Kügelgen, Hamed Hassani, George J Pappas, and Bernhard Schölkopf. Probable domain generalization via quantile risk minimization. *arXiv preprint arXiv:2207.09944*, 2022. 3
- [9] Kaiming He, Xiangyu Zhang, Shaoqing Ren, and Jian Sun. Deep residual learning for image recognition. In *Proceedings of the IEEE Conference on Computer Vision and Pattern Recognition (CVPR)*, pages 770–778, 2016. 3
- [10] Kaiming He, Xiangyu Zhang, Shaoqing Ren, and Jian Sun. Deep residual learning for image recognition. In *Proceedings of the IEEE conference on computer vision and pattern recognition (CVPR)*, pages 770–778, 2016. 5, 7
- [11] Yihui He, Xiangyu Zhang, and Jian Sun. Channel pruning for accelerating very deep neural networks. In *Proceedings of the IEEE International Conference on Computer Vision (ICCV)*, pages 1389–1397, 2017. 3
- [12] Lei Huang, Dawei Yang, Bo Lang, and Jia Deng. Decorrelated batch normalization. In *Proceedings of the IEEE Conference on Computer Vision and Pattern Recognition (CVPR)*, pages 791–800, 2018. 3, 5
- [13] Xun Huang and Serge Belongie. Arbitrary style transfer in real-time with adaptive instance normalization. In *Proceedings of the IEEE International Conference on Computer vision (CVPR)*, pages 1501–1510, 2017. 3
- [14] Zeyi Huang, Haohan Wang, Eric P Xing, and Dong Huang. Self-challenging improves cross-domain generalization. In *Proceedings of the European Conference on Computer Vision (ECCV)*, pages 124–140, 2020. 6
- [15] Nitish Shirish Keskar, Dheevatsa Mudigere, Jorge Nocedal, Mikhail Smelyanskiy, and Ping Tak Peter Tang. On large-batch training for deep learning: Generalization gap and sharp minima. *arXiv preprint arXiv:1609.04836*, 2016. 8
- [16] Pang Wei Koh, Shiori Sagawa, Henrik Marklund, Sang Michael Xie, Marvin Zhang, Akshay Balsubramani, Weihua Hu, Michihiro Yasunaga, Richard Lanus Phillips, Irena Gao, et al. Wilds: A benchmark of in-the-wild distribution shifts. In *Proceedings of the International Conference on Machine Learning (ICML)*, pages 5637–5664, 2021. 6
- [17] Da Li, Yongxin Yang, Yi-Zhe Song, and Timothy Hospedales. Learning to generalize: Meta-learning for domain generalization. In *Proceedings of the AAAI conference on Artificial Intelligence*, volume 32, 2018. 3
- [18] Da Li, Yongxin Yang, Yi-Zhe Song, and Timothy M Hospedales. Deeper, broader and artier domain generalization. In *Proceedings of the IEEE International Conference on Computer Vision (ICCV)*, pages 5542–5550, 2017. 2, 5
- [19] Haoliang Li, Sinno Jialin Pan, Shiqi Wang, and Alex C Kot. Domain generalization with adversarial feature learning. In *Proceedings of the IEEE Conference on Computer Vision and Pattern Recognition (CVPR)*, pages 5400–5409, 2018. 3
- [20] Haoliang Li, YuFei Wang, Renjie Wan, Shiqi Wang, Tie-Qiang Li, and Alex Kot. Domain generalization for medical imaging classification with linear-dependency regularization. *Advances in Neural Information Processing Systems*, 33:3118–3129, 2020. 2, 3
- [21] Xiaotong Li, Yongxing Dai, Yixiao Ge, Jun Liu, Ying Shan, and LINGYU DUAN. Uncertainty modeling for out-of-distribution generalization. In *International Conference on Learning Representations*, 2022. 1, 3, 4, 6, 7
- [22] Quande Liu, Cheng Chen, Jing Qin, Qi Dou, and Pheng-Ann Heng. Feddg: Federated domain generalization on medical image segmentation via episodic learning in continuous frequency space. In *Proceedings of the IEEE/CVF Conference on Computer Vision and Pattern Recognition (CVPR)*, pages 1013–1023, 2021. 2
- [23] Wang Lu, Jindong Wang, Haoliang Li, Yiqiang Chen, and Xing Xie. Domain-invariant feature exploration for domain generalization. *arXiv preprint arXiv:2207.12020*, 2022. 2, 3
- [24] Hyeonseob Nam and Hyo-Eun Kim. Batch-instance normalization for adaptively style-invariant neural networks. *Advances in Neural Information Processing Systems (NIPS)*, 31, 2018. 4
- [25] Hyeonseob Nam, HyunJae Lee, Jongchan Park, Wonjun Yoon, and Donggeun Yoo. Reducing domain gap by reducing style bias. In *Proceedings of the IEEE/CVF Conference on Computer Vision and Pattern Recognition (CVPR)*, pages 8690–8699, 2021. 6

- [26] Oren Nuriel, Sagie Benaïm, and Lior Wolf. Permuted adain: Reducing the bias towards global statistics in image classification. In *Proceedings of the IEEE/CVF Conference on Computer Vision and Pattern Recognition (CVPR)*, pages 9482–9491, 2021. 3, 4, 6, 7
- [27] Adam Paszke, Sam Gross, Francisco Massa, Adam Lerer, James Bradbury, Gregory Chanan, Trevor Killeen, Zeming Lin, Natalia Gimelshein, Luca Antiga, et al. Pytorch: An imperative style, high-performance deep learning library. *Advances in NIPS*, 32, 2019. 5
- [28] Viraj Prabhu, Shivam Khare, Deeksha Kartik, and Judy Hoffman. Sentry: Selective entropy optimization via committee consistency for unsupervised domain adaptation. In *Proceedings of the IEEE/CVF International Conference on Computer Vision (CVPR)*, pages 8558–8567, 2021. 1
- [29] Fengchun Qiao, Long Zhao, and Xi Peng. Learning to learn single domain generalization. In *Proceedings of the IEEE/CVF Conference on Computer Vision and Pattern Recognition (CVPR)*, pages 12556–12565, 2020. 2
- [30] Ergys Ristani, Francesco Solera, Roger Zou, Rita Cucchiara, and Carlo Tomasi. Performance measures and a data set for multi-target, multi-camera tracking. In *Proceedings of the European conference on computer vision (ECCV)*, pages 17–35, 2016. 2, 7
- [31] Kuniaki Saito, Donghyun Kim, Stan Sclaroff, Trevor Darrell, and Kate Saenko. Semi-supervised domain adaptation via minimax entropy. In *Proceedings of the IEEE/CVF International Conference on Computer Vision (CVPR)*, pages 8050–8058, 2019. 1
- [32] Shiv Shankar, Vihari Piratla, Soumen Chakrabarti, Siddhartha Chaudhuri, Preethi Jyothi, and Sunita Sarawagi. Generalizing across domains via cross-gradient training. *arXiv preprint arXiv:1804.10745*, 2018. 6
- [33] Yang Shu, Zhangjie Cao, Chenyu Wang, Jianmin Wang, and Mingsheng Long. Open domain generalization with domain-augmented meta-learning. In *Proceedings of the IEEE/CVF Conference on Computer Vision and Pattern Recognition (CVPR)*, pages 9624–9633, 2021. 3
- [34] Hemanth Venkateswara, Jose Eusebio, Shayok Chakraborty, and Sethuraman Panchanathan. Deep hashing network for unsupervised domain adaptation. In *Proceedings of the IEEE Conference on Computer Vision and Pattern Recognition (CVPR)*, pages 5018–5027, 2017. 2, 6
- [35] Vikas Verma, Alex Lamb, Christopher Beckham, Amir Najafi, Ioannis Mitliagkas, David Lopez-Paz, and Yoshua Bengio. Manifold mixup: Better representations by interpolating hidden states. In *Proceedings of the ICML*, pages 6438–6447, 2019. 6
- [36] Riccardo Volpi, Hongseok Namkoong, Ozan Sener, John C Duchi, Vittorio Murino, and Silvio Savarese. Generalizing to unseen domains via adversarial data augmentation. *Advances in Neural Information Processing Systems ((NIPS))*, 31, 2018. 2
- [37] Yoav Wald, Amir Feder, Daniel Greenfeld, and Uri Shalit. On calibration and out-of-domain generalization. *Advances in Neural Information Processing Systems*, 34:2215–2227, 2021. 3
- [38] Jindong Wang, Cuiling Lan, Chang Liu, Yidong Ouyang, Tao Qin, Wang Lu, Yiqiang Chen, Wenjun Zeng, and Philip Yu. Generalizing to unseen domains: A survey on domain generalization. *IEEE Transactions on Knowledge and Data Engineering*, 2022. 2
- [39] Zhenlin Xu, Deyi Liu, Junlin Yang, Colin Raffel, and Marc Niethammer. Robust and generalizable visual representation learning via random convolutions. *arXiv preprint arXiv:2007.13003*, 2020. 2, 6
- [40] Sangdoo Yun, Dongyoon Han, Seong Joon Oh, Sanghyuk Chun, Junsuk Choe, and Youngjoon Yoo. Cutmix: Regularization strategy to train strong classifiers with localizable features. In *Proceedings of the IEEE/CVF International Conference on Computer Vision (CVPR)*, pages 6023–6032, 2019. 6
- [41] Hongyi Zhang, Moustapha Cisse, Yann N Dauphin, and David Lopez-Paz. mixup: Beyond empirical risk minimization. *arXiv preprint arXiv:1710.09412*, 2017. 6
- [42] Ling Zhang, Xiaosong Wang, Dong Yang, Thomas Sanford, Stephanie Harmon, Baris Turkbey, Bradford J Wood, Holger Roth, Andriy Myronenko, Daguang Xu, et al. Generalizing deep learning for medical image segmentation to unseen domains via deep stacked transformation. *IEEE Transactions on Medical Imaging*, 39(7):2531–2540, 2020. 2
- [43] Shengdong Zhang, Ehsan Nezhadarya, Homa Fashandi, Jiayi Liu, Darin Graham, and Mohak Shah. Stochastic whitening batch normalization. In *Proceedings of the IEEE/CVF Conference on Computer Vision and Pattern Recognition (CVPR)*, pages 10978–10987, 2021. 3
- [44] Shanshan Zhao, Mingming Gong, Tongliang Liu, Huan Fu, and Dacheng Tao. Domain generalization via entropy regularization. *Advances in Neural Information Processing Systems (NIPS)*, 33:16096–16107, 2020. 3
- [45] Liang Zheng, Liye Shen, Lu Tian, Shengjin Wang, Jingdong Wang, and Qi Tian. Scalable person re-identification: A benchmark. In *Proceedings of the IEEE International Conference on Computer Vision (ECCV)*, pages 1116–1124, 2015. 2, 7
- [46] Zhun Zhong, Liang Zheng, Guoliang Kang, Shaozi Li, and Yi Yang. Random erasing data augmentation. In *Proceedings of the AAAI Conference on Artificial Intelligence*, volume 34, pages 13001–13008, 2020. 7
- [47] Kaiyang Zhou, Ziwei Liu, Yu Qiao, Tao Xiang, and Chen Change Loy. Domain generalization: A survey. *IEEE Transactions on Pattern Analysis and Machine Intelligence*, 2022. 1, 2, 5
- [48] Kaiyang Zhou, Yongxin Yang, Timothy Hospedales, and Tao Xiang. Learning to generate novel domains for domain generalization. In *Proceedings of the European conference on computer vision (ECCV)*, pages 561–578, 2020. 6, 7
- [49] Kaiyang Zhou, Yongxin Yang, Yu Qiao, and Tao Xiang. Domain generalization with mixstyle. *arXiv preprint arXiv:2104.02008*, 2021. 1, 3, 4, 6, 7, 8

Supplementary Materials

The supplementary materials provide the pseudo-code for implementing the Correlated Style Uncertainty (CSU) model. To guarantee the reliability of reporting results, we also conduct training stability analysis on PACS dataset. We conduct an ablation experiment to analyze the position selection effects on the Duke-Market1501 instance retrieval task. Furthermore, we visualize the extracted feature using t-SNE projection, which proves that CSU can help with extracting domain-invariant feature representations.

1. Pseudo Code

Here, we provide the pseudo-code for our CSU model. As we can observe, this code is relatively easy to implement and can be encoded into most current models. Note that we do not use the backpropagation of the normal PyTorch Eigh function for eigenvalue decomposition to avoid instability during training. This is because the gradient calculation relies on the smallest value of the eigenvalue difference $\frac{1}{\min(\lambda_i - \lambda_j)}$.

```
# Given eps, alpha, p=0.5
# Input: x:B*C*H*W
# Output: x:B*C*H*W
def decompose(matrix):
    with torch.no_grad():
        value, vect = eigh(matrix)
        lmda = sqrt(vect.T@matrix@vect)
    return vect@lmda@vect.T

def forward(x):
    if random < p:
        return x
    mu = mean(x, dim=(2, 3))
    sig = std(x, dim=(2, 3)) + eps
    x_norm = (x - mu) / sig
    corr_mu = decompose(mu.T@mu)
    corr_sig = decompose(sig.T@sig)
    rand_mu = randn_like(mu)@corr_mu
    rand_sig = randn_like(sig)@corr_sig
    inten = Beta(alpha, alpha).sample(N, 1)
    mu = mu + inten*rand_mu
    sig = sig + inten*rand_sig
    x = mu + x_norm*sig
    return x
```

Listing 1. An Pytorch-like pseudo code for CSU

This can induce extremely unstable training, considering that we have many zero eigenvalues, as described in the previous section. We assume that the direction is relatively

stable during the training to address this issue. The key for backpropagation is calculating the eigenvalue or variance intensity for the corresponding direction. Thus, we adopt an algorithm that does not pass the gradient through the eigenvector. We show the pseudo implementation in 1

2. Training Reliability

We conduct the training process using the exact configuration on the PACS dataset multi-time. Here we set $\alpha = 0.3$. We perform 20 times of experiments and calculate the performance distribution to test the training stability. The standard deviations of Art, Cartoon, Photo, and Sketch are 0.35, 0.17, 0.12, and 0.30, respectively, and the standard deviation of Average is 0.13. Figure 1 shows the result. We can observe that the standard deviation is relatively low, and the One-Sigma range is (84.90, 85.17), which indicates that the training process is consistent and reliable.

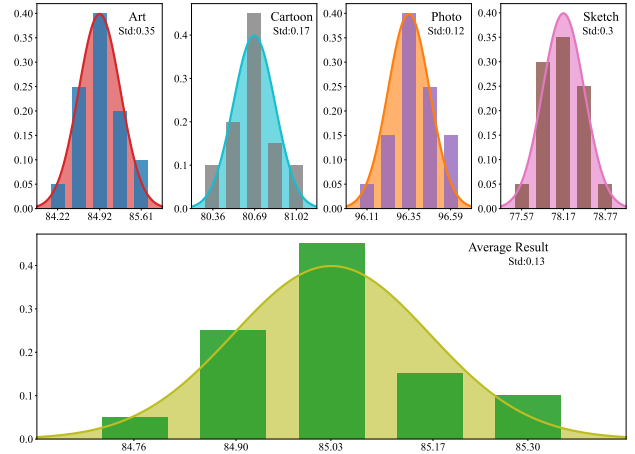


Figure 1. One visualization of training stability. We perform 20 times of experiments and calculate the standard deviations of each category and the average performance. We can observe that the training is stable given the low standard deviation value.

3. Position Selection For Instance Retrieval

We conduct an ablation experiment to analyze the position selection effects on the Duke-Market1501 instance retrieval task. Here we show the influence of different insert-

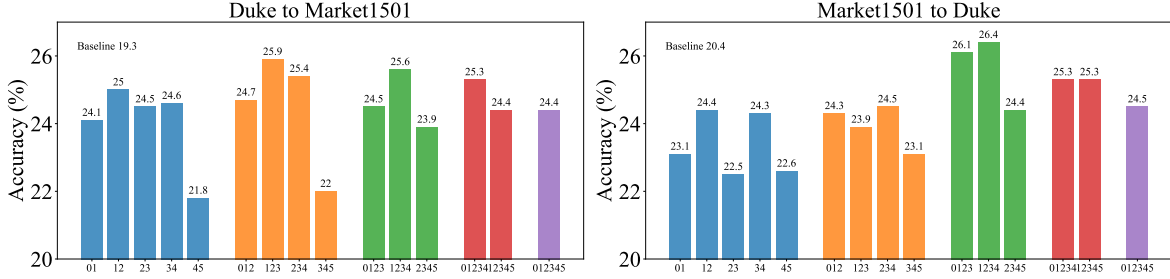


Figure 2. One visualization of different inserting positions on the instance retrieval experiments. We can achieve better performance than reporting by changing the inserting position. This shows the best position configuration might vary by task rather than one fixed conclusion.

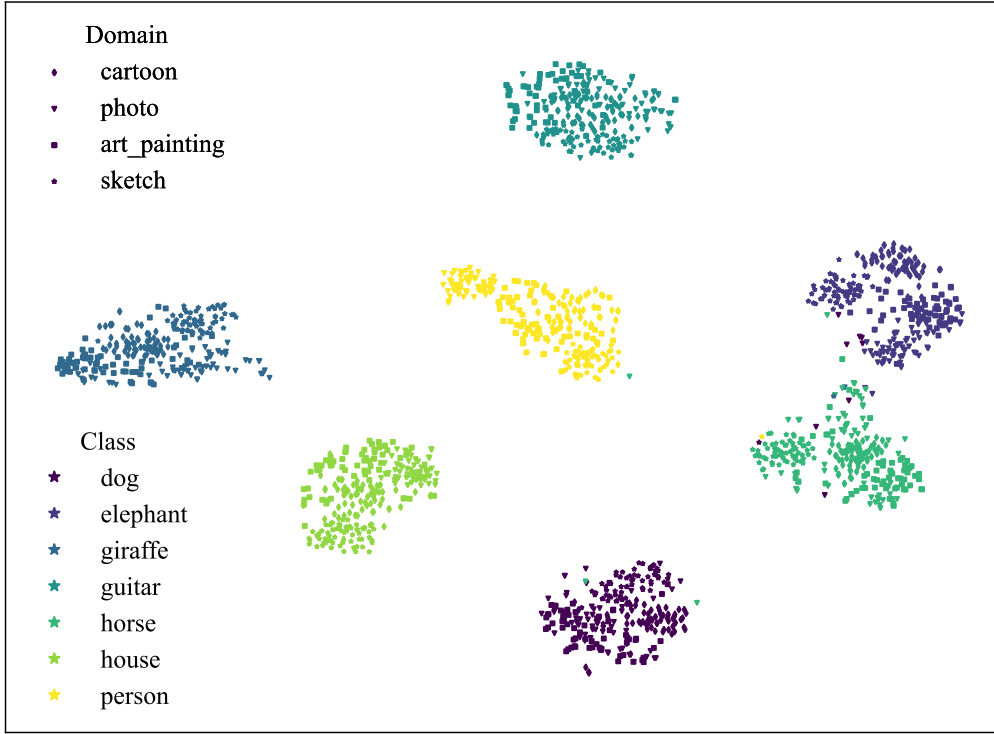


Figure 3. 2-D Visualization of Flattened Feature Maps. We can clearly observe that the trained model can effectively obtain more domain-invariant feature representations. For 4 domains of the PACS dataset, including Art, Cartoon, Photo, and Sketch, we select 64 cases from every category (7 categories in total) under each domain.

ing positions in Figure 2. We can find that overall trends are similar to the classification tasks. Notably, we can achieve impressive improvement compared to the reported result (the "012345" group) by changing position. This indicates that the best position configuration may vary by task rather than one fixed conclusion.

4. Visualization of Flattened Feature Maps

To intuitively understand the effectiveness of our method, we provide the t-SNE visualization map of feature vectors extracted from the trained model. As shown in Figure 3, we can find that with the CSU, the distance between different domains within the same category is small, while the distance between different classes, regardless of the do-

main, is immense. Therefore, we can show that the trained model can obtain more domain-invariant feature representations, indicating a more vital generalization ability.